

Supporting information

Synthesis and characterization of magnetic mesoporous nanoparticles Fe₃O₄@mSiO₂- DODGA for adsorption of 16 rare earth elements

Jingrui Li^{a,b}, Aijun Gong^{a,b*}, Fukai Li^{a,b}, Lina Qiu^{a,b}, Weiwei Zhang^{a,b},

Ge Gao^{a,b}, Yu Liu^{a,b}, Jiandi Li^{a,b}

a. School of chemistry and biological engineering, University of Science and Technology Beijing,
Beijing 100083, China

b. Beijing Key Laboratory for Science and Application of Functional Molecular and Crystalline Materials,
University of Science and Technology Beijing, Beijing 100083, China

Corresponding Author

* Email: Gongaijun5661@ustb.edu.cn. Tel: (+86) 010-82375661. Fax: (+86) 010-62334071

Figure S1. The mass spectra of DODGA	2
Figure S2. The mass spectra of glycolic anhydride	2
Figure S3. The ¹ H NMR spectra of DODGA	3
Figure S4. The ¹ H NMR spectra of glycolic anhydride	3
Figure S5. The ¹³ C NMR spectra of DODGA	4
Figure S6. The ¹³ C NMR spectra of glycolic anhydride	4
Table S1. The pseudo-first order kinetic model	5
Table S2. The pseudo-second-order model	5
Table S3. The intra-particle diffusion model	6
Table S4. The Elovich model	6
Table S5. The Langmuir model	7
Table S6. The Freundlich model	8
Table S7. The Tempkin model	8
Table S8. The D-R model	9
Table S9. 16 kinds of REEs linear standard curve	10
Table S10. Comparison of the Fe ₃ O ₄ @mSiO ₂ -DODGA with the other conventional materials	12
Figure S8. The pore diameter of Fe ₃ O ₄ @mSiO ₂ -DODGA	12
Figure S9. The pore structure of Fe ₃ O ₄ @SiO ₂	12

Material preparation

Synthesis of $\text{Fe}_3\text{O}_4@m\text{SiO}_2@\text{NH}_2$

Fe_3O_4 magnetic nanoparticles were synthesized by solvothermal reaction according to the literature¹. Typically, FeCl_3 (6 m mol, 1.62 g) and carbamide (30 m mol, 1.80 g) were dissolved in ethylene glycol (58mL) and water (2mL). The obtained mixture was stirred vigorously at room temperature for 30 min and added subsequently into a Teflon-lined stainless autoclave. The autoclave was sealed and placed in a muffle furnace. The increasing temperature programmed was set from room temperature to 200 °C in 1 h and remained 200 °C for 16 h, followed by cooling to room temperature. The black precipitate was collected by an external magnetic field and purified by washing sequentially with ethanol and ultrapure water for three times, respectively.

The $\text{Fe}_3\text{O}_4@\text{SiO}_2$ particles were synthesized according to the reported method^{2,3}. Briefly, Fe_3O_4 magnetic nanoparticles (0.3 g) was added into a mixed solution of ethanol (160 mL) and ultrapure water (40 mL). The dispersion mixture was sonicated for 30 min to make the nanoparticles disperse evenly. After that, the concentrated ammonia aqueous solution (5 mL, 25 wt%) and TEOS (3.1 m mol, 0.7 mL) was added to make sol-gel reaction occurred on the surface of the particles. The mixture was stirring for 8 h at 40 °C. Finally, the $\text{Fe}_3\text{O}_4@\text{SiO}_2$ particles were separated and washed with ethanol and ultrapure water respectively, dried under vacuum.

The mesoporous SiO_2 layer coated on SiO_2 shell was prepared with the following method. Typically, $\text{Fe}_3\text{O}_4@\text{SiO}_2$ particles (0.4 g) was added into a mixed solution of ethanol (30 mL) and ultrapure water (20 mL). The dispersion mixture was sonicated for 10 min. the concentrated ammonia aqueous solution (1 mL, 28 wt%), CTAB(0.9 g) and TEOS (9 mmol, 2.0 mL) was added subsequently. The mixture was stirring for 10 h at room temperature. The $\text{Fe}_3\text{O}_4@m\text{SiO}_2$ particles were separated and washed with ethanol and ultrapure water. To remove CTAB⁴, the obtained $\text{Fe}_3\text{O}_4@m\text{SiO}_2$ particles were added into a mixed solution of ethanol (150 mL) and $\text{NH}_4\cdot\text{NO}_3$ (0.9 g). The mixture was refluxed for 3 h.

Amine functionalization nanoparticles $\text{Fe}_3\text{O}_4@m\text{SiO}_2@\text{NH}_2$ were prepared by reacting with APTES⁵. Briefly, anhydrous toluene (50 mL) and $\text{Fe}_3\text{O}_4@m\text{SiO}_2$ particles (0.4 g) were added in a three-neck flask. The mixture was sonicated for 30min to make the particles disperse. APTES (4 mL) was added into the flask. The reaction was going on under nitrogen gas protection at 120 °C for 24 h. The resultant $\text{Fe}_3\text{O}_4@m\text{SiO}_2@\text{NH}_2$ nanoparticles were washed with anhydrous toluene and acetone for three times, respectively, and dried under vacuum.

Synthesis of DODGA-Cl

The synthesis of DODGA-Cl was referred the literature^{6,7}. Diglycolic acid (37.3 mM, 5.0 g) was dissolved in acid anhydride (132.2 mM, 12.5mL) under a nitrogen atmosphere. The mixture was stirred and heated to reflux. After refluxing for 10 min, 3 drops of

phosphoric acid were added into the reaction mixture to catalysis the reaction. The solution was stirred under reflux conditions for 2 hour. The resulting solution was concentrated through rotary evaporation under reduced pressure. The final solution was poured into the toluene to recrystallize the products. After filtrating the solid generated in toluene, a white needle-like product (3.6 g, 83% yield) was obtained to be used directly in the next synthesis step.

In the second step⁸, didoethylamine (16.0 m mol, 3.86 g) was placed in a 250 ml round bottom flask and dissolved in DCM (150 ml), glycolic anhydride (22.4 m mol, 2.62 g) was added, and the mixture was stirred at room temperature for 2 h. The end of the reaction was controlled by TLC (DCM/MeOH 8:2). The mixture was concentrated; and the residue was taken up in ethyl acetate, washed successively with 0.1N HCl (×2) and sat. NaCl, and dried over Na₂SO₄. Evaporation of the solvent gave the title compound as an oil which crystallized on standing (5.00 g, 87.5%).

Converting the DODGA-OH to its acyl chloride derivative was referred the normal organic reaction operation. Typically, DODGA-OH (10 m mol, 3.60 g) was dissolved in the solvent of CH₂Cl₂ (30 mL). Anhydrous oxalyl chloride(15 m mol, 1.3mL) was added into the mixture. After stirring for 10 min, 2 drops of DMF was added to catalyze the reaction. The reaction was monitored by thin layer chromatography. At the end of the reaction, the solvent and excessive oxalyl chloride was removed by rotary evaporating. The residue was DODGA-Cl (3.30 g, 87.2%) that could be used directly to modify magnetic particles.

Modifying the Fe₃O₄ particles with the functional unit of DODGA

The functionalized Fe₃O₄ particles were prepared by the reaction between the anime groups on the surface of the Fe₃O₄@mSiO₂@NH₂ and the DODGA-Cl. Briefly, the Fe₃O₄@mSiO₂@NH₂(0.3 g) and TEA(15 m mol, 2.1 mL) was added into the solvent of anhydrous CH₂Cl₂ (30 mL). The mixture was sonicated for 15min. the solution of DODGA-Cl (10 m mol, 3.75 g) in anhydrous CH₂Cl₂ (10 mL) was dropped slowly into the mixture. The reaction was going on at room temperature for 8 h. The resultant particles were washed with CH₂Cl₂ and methanol three times respectively, and dried under vacuum.

TOGDA #13 RT: 0.20 AV: 1 NL: 1.45E5
T: ITMS + c ESI Full ms [110.00-500.00]

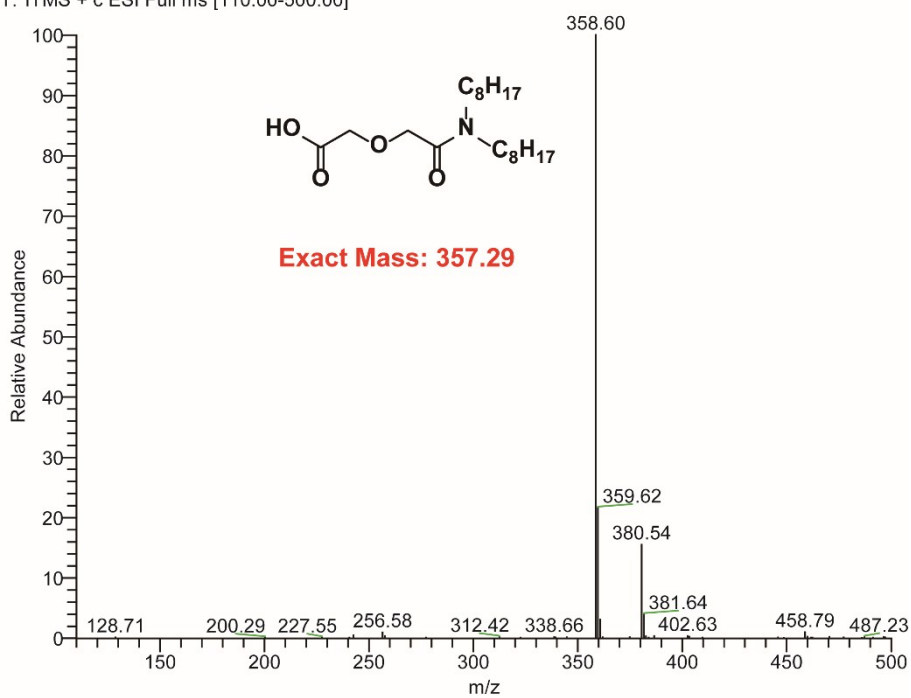


Figure S1. The mass spectra of DODGA

二甘醇酸 #13 RT: 0.21 AV: 1 NL: 7.13E3
T: ITMS + c ESI Full ms [110.00-150.00]

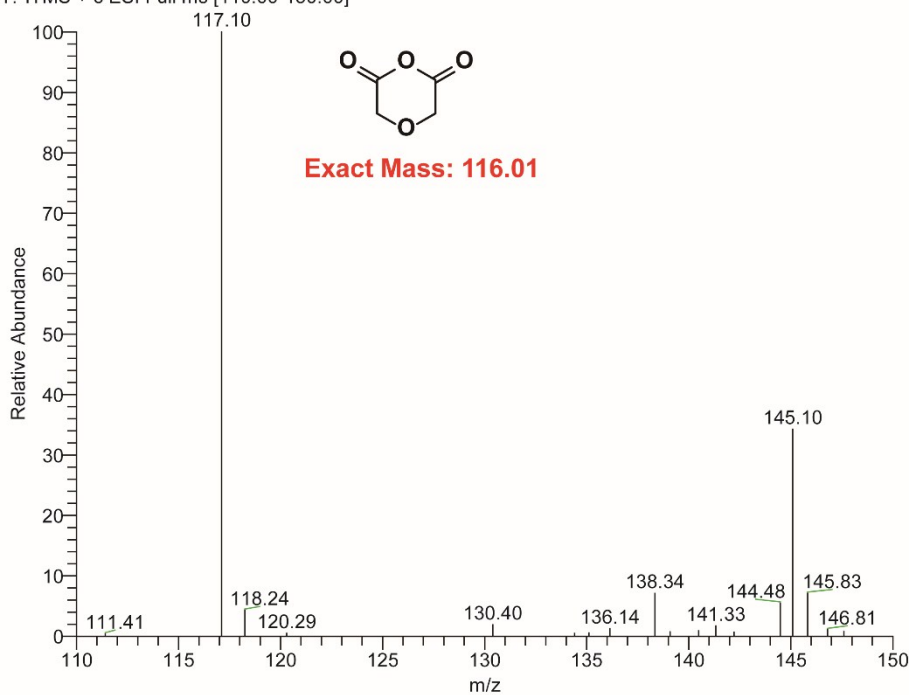


Figure S2. The mass spectra of Glycolic anhydride

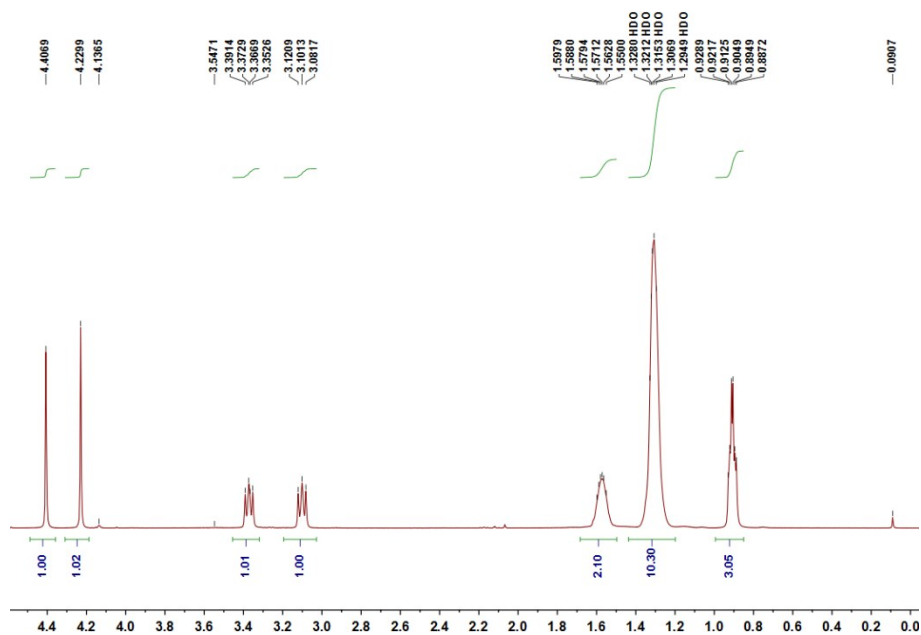


Figure S3. The ^1H NMR spectra of DODGA
 ^1H NMR (400 MHz, Chloroform-*d*) δ 4.41 (s, 1H), 4.23 (s, 1H), 3.37 (dd, $J = 9.0, 6.6$ Hz, 1H), 3.19-3.03 (m, 1H), 1.68-1.50 (m, 2H), 1.31 (s, 10H), 0.91 (td, $J = 6.8, 3.0$ Hz, 3H).

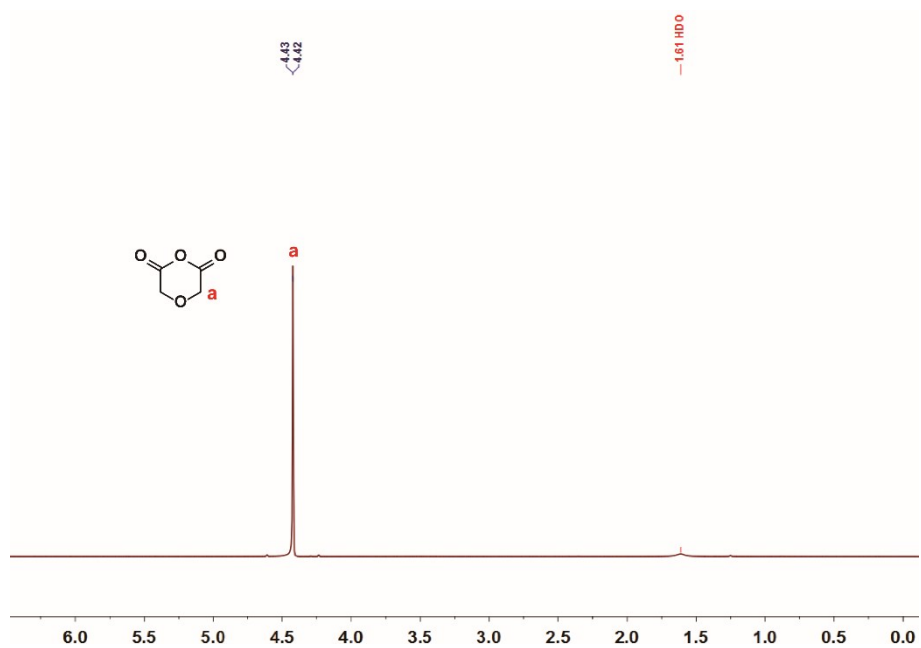


Figure S4. The ^1H NMR spectra of Glycolic anhydride
 ^1H NMR (400 MHz, Chloroform-*d*) δ 4.42 (d, $J = 1.4$ Hz, 4H).

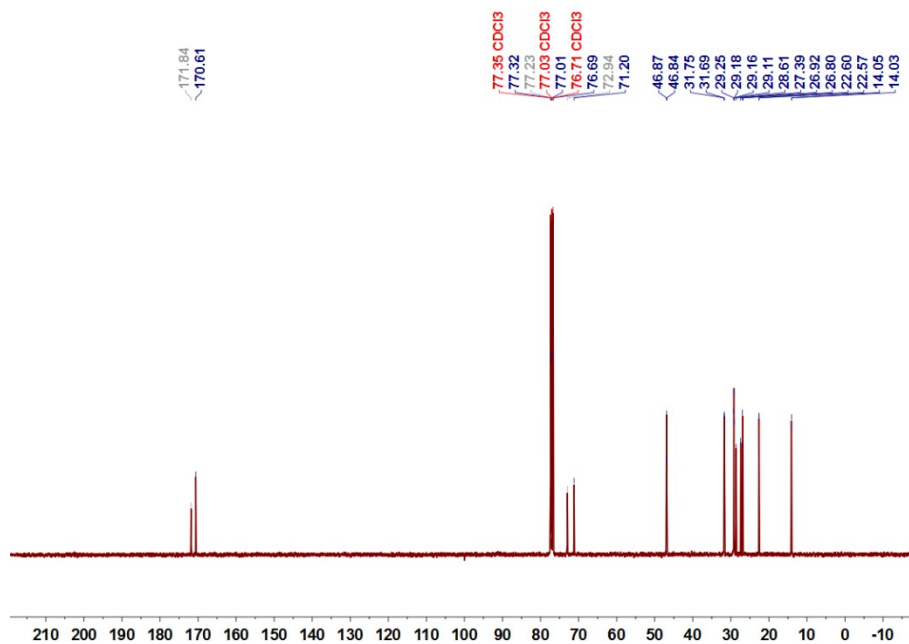


Figure S5. The ^{13}C NMR spectra of DODGA

^{13}C NMR (101 MHz, CDCl_3) δ 171.84, 170.61, 72.94, 71.20, 46.87, 46.84, 31.75, 31.69, 29.25, 29.18, 29.16, 29.11, 28.61, 27.39, 26.92, 26.80, 22.60, 22.57, 14.05, 14.03. MS (ESI): calcd. for $\text{C}_{20}\text{H}_{39}\text{NO}_4$: 357.29; found:358.60.

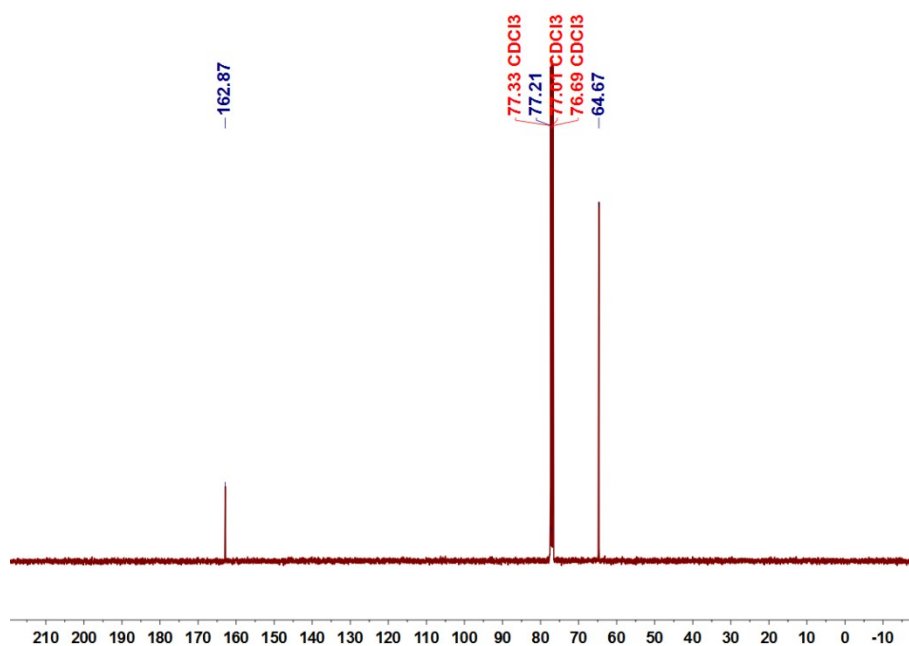


Figure S6. The ^{13}C NMR spectra of Glycolic anhydride

^{13}C NMR (101 MHz, Chloroform-*d*) δ 162.87, 64.67. MS (ESI): calcd. for $\text{C}_4\text{H}_4\text{O}_4$: 116.01; found:117.10.

Adsorption kinetics

Pseudo-first order kinetic model⁹

$$q_t = q_e(1 - e^{-k_1 t})$$

Where $q_e(\text{mg}\cdot\text{g}^{-1})$ and $q_t(\text{mg}\cdot\text{g}^{-1})$ refer to the amounts of REEs adsorbed at equilibrium and designed time, respectively. $k_1(\text{min}^{-1})$ Pseudo-first order reaction rate constant.

Table S1. The result of data processing according to pseudo-first order kinetic model

Elements	Equation	Parameter		
		R ²	q _e mg·g ⁻¹	k ₁ min ⁻¹
Nd	q _t =57.36(1-e ^{-0.089t})	0.9000	57.362	0.0891
Sm	q _t =26.65(1-e ^{-0.066t})	0.9755	26.6529	0.0665
Eu	q _t =35.40(1-e ^{-0.188t})	0.7948	35.3960	0.1882
Ho	q _t =16.43(1-e ^{-0.093t})	0.9561	16.428	0.0927
Yb	q _t =33.16(1-e ^{-0.105t})	0.9761	33.1592	0.1052
Lu	q _t =39.29(1-e ^{-0.285t})	0.5491	39.2897	0.2851
Y	q _t =15.60(1-e ^{-0.103t})	0.9592	15.6051	0.1032
Sc	q _t =13.85(1-e ^{-0.088t})	0.9106	13.8479	0.0881

Pseudo-second-order model¹⁰

$$\frac{t}{q_t} = \frac{1}{2k_2 q_e^2} + \frac{1}{q_e} t$$

Where k_2 was pseudo-second-order reaction rate constant ($\text{g}\cdot\text{mg}^{-1}\cdot\text{min}^{-1}$), the initial adsorption rate $h(\text{mg}\cdot\text{g}^{-1}\cdot\text{min}^{-1})$ was calculated from the following equation: $h=k_2 q_e^2$

Table S2. The result of data processing according to pseudo-second-order model

Elements	Equation	Parameter		
		R ²	q _e mg·g ⁻¹	k ₂ g·mg ⁻¹ ·min ⁻¹
Nd	t/q _t =0.1484+0.0162t	0.9997	61.7584	282.7313
Sm	t/q _t =0.3136+0.0357t	0.9998	28.0112	123.0296
Eu	t/q _t =0.0828+0.027t	1.0000	37.0370	56.7901
Ho	t/q _t =0.4107+0.0578t	0.9997	17.3010	61.4666
Yb	t/q _t =0.1515+0.0289t	0.9999	34.6021	90.6958
Lu	t/q _t =0.095+0.0237t	0.9998	42.1941	84.5662
Y	t/q _t =0.3802+0.0608t	0.9999	16.4474	51.4251
Sc	t/q _t =0.5058+0.0687t	0.9997	14.5560	53.5840

Intra-particle diffusion model¹¹

$$q_t = k_i t^{1/2} + C$$

Where k_i was intra-particle diffusion rate constant ($\text{mg} \cdot \text{g}^{-1} \cdot \text{min}^{-1/2}$), C represented the boundary layer diffusion effect. The larger the value of C , the greater the diffusion effect of the boundary layer.

Table S3. The result of data processing according to intra-particle diffusion model

Elements	Equation	Parameter		
		R ²	k_i $\text{mg} \cdot \text{g}^{-1} \cdot \text{min}^{-1/2}$	C
Nd	$q_t = 35.996 + 1.4109 t^{1/2}$	0.6592	1.4109	35.996
Sm	$q_t = 14.789 + 0.7398 t^{1/2}$	0.5851	0.7398	14.789
Eu	$q_t = 28.686 + 0.4675 t^{1/2}$	0.5898	0.4675	28.686
Ho	$q_t = 10.433 + 0.3864 t^{1/2}$	0.4838	0.3864	10.433
Yb	$q_t = 22.532 + 0.6897 t^{1/2}$	0.5001	0.6897	22.532
Lu	$q_t = 33.574 + 0.4466 t^{1/2}$	0.8311	0.4466	33.574
Y	$q_t = 10.419 + 0.3384 t^{1/2}$	0.4985	0.3384	10.419
Sc	$q_t = 8.7572 + 0.3277 t^{1/2}$	0.4386	0.3277	8.7572

Elovich model¹²

$$q_t = \frac{\ln(\alpha\beta)}{\beta} + \frac{\ln t}{\beta}$$

Where α ($\text{mg} \cdot \text{g}^{-1} \cdot \text{min}^{-1}$) was the initial adsorption rate constant, β ($\text{mg} \cdot \text{g}^{-1} \cdot \text{min}^{-1}$) was a parameter related to the surface coverage of the adsorbent and the activation energy of chemical adsorption.

Table S4. The result of data processing according to Elovich model

Elements	Equation	Parameter		
		R ²	α $\text{mg} \cdot \text{g}^{-1} \cdot \text{min}^{-1}$	β $\text{mg} \cdot \text{g}^{-1} \cdot \text{min}^{-1}$
Nd	$q_t = 26.945 \ln t + 14.218$	0.9612	45.6711	0.03711
Sm	$q_t = 14.724 \ln t + 2.5879$	0.9266	17.5533	0.06792
Eu	$q_t = 9.2842 \ln t + 21.003$	0.9298	89.1700	0.10771
Ho	$q_t = 8.2165 \ln t + 3.3692$	0.8744	12.38142	0.12171
Yb	$q_t = 14.55 \ln t + 10.074$	0.8899	29.0774	0.06873
Lu	$q_t = 7.696 \ln t + 27.774$	0.9867	284.1745	0.12994
Y	$q_t = 7.1041 \ln t + 4.3537$	0.8782	13.1118	0.14076
Sc	$q_t = 7.0795 \ln t + 4.3537$	0.8181	13.0943	0.14125

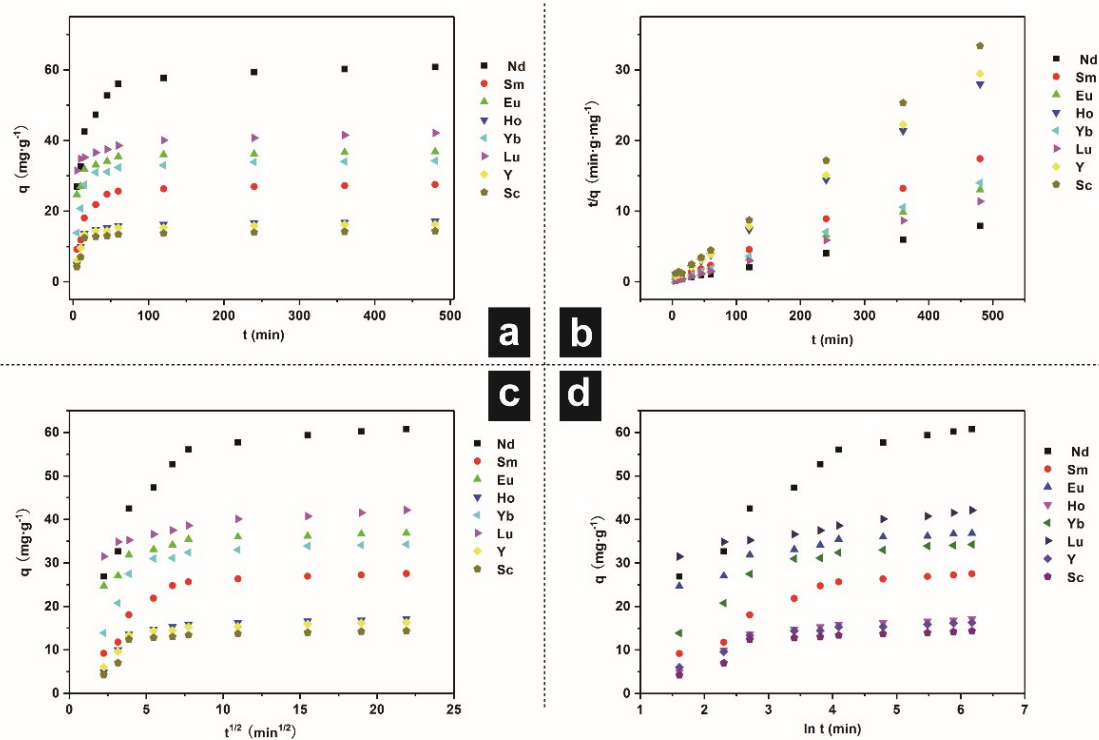


Figure S7. Different adsorption kinetic model of Fe₃O₄@ mSiO₂-TODGA for REEs (a. pseudo-first-order, b. pseudo-second-order, c. intra-particle diffusion, d. Elovich model)

Adsorption isotherms

Langmuir model¹³

$$\frac{C_e}{q_e} = \frac{C_e}{Q_{max}} + \frac{1}{K_L Q_{max}}$$

Where $Q_e(\text{mg}\cdot\text{g}^{-1})$ and $C_e(\text{mg}\cdot\text{L}^{-1})$ was the amount of nanoparticles adsorbed and the concentration of REEs in the solution under the equilibrium, respectively; $Q_{max}(\text{mg}\cdot\text{g}^{-1})$ was the saturated monolayer adsorption, and $K_L(\text{L}\cdot\text{mg}^{-1})$ was the Langmuir constant, which is related to the binding energy of the adsorption system.

Table S5. The result of data processing according to Langmuir model

Elements	Equation	Parameter			
		R ²	Q _{max} (mg·g ⁻¹)	K _L (L·mg ⁻¹)	R _L
Nd	$C_e/q_e=0.0145 C_e +0.0109$	0.9327	68.9655	1.3303	0.4291
Sm	$C_e/q_e=0.0350 C_e +0.0102$	0.9987	28.5714	3.4314	0.2256
Eu	$C_e/q_e=0.0249 C_e +0.0211$	0.9981	40.1606	1.1801	0.4586
Ho	$C_e/q_e=0.0579 C_e +0.0439$	0.9892	17.2712	1.3189	0.4312
Yb	$C_e/q_e=0.0258 C_e +0.0236$	0.9911	38.7597	1.0932	0.4777
Lu	$C_e/q_e=0.022 C_e +0.0222$	0.9900	45.4545	0.9910	0.5022
Y	$C_e/q_e=0.0568 C_e +0.0318$	0.9919	17.6056	1.7862	0.3589
Sc	$C_e/q_e=0.0674 C_e +0.0105$	0.9983	14.8368	6.4190	0.1347

Freundlich model¹⁴

$$\ln(Q_e) = \ln(K_f) + \frac{1}{n} \ln(C_e)$$

where K_f and n was the Freundlich isotherm constant, respectively. K_f was related to the adsorption amount, and n was related to the strength of the adsorption. The value of $1/n$ between 0.1-0.5 indicated that the adsorption process was favorable.

Table S6. The result of data processing according to Freundlich model

Elements	Equation	Parameter		
		R ²	K _f	n
Nd	$\ln(q_e)=0.4574\ln(C_e)+3.4593$	0.9972	31.7947	2.1863
Sm	$\ln(q_e)=0.2941\ln(C_e)+2.7919$	0.9366	16.3120	3.4002
Eu	$\ln(q_e)=0.1542\ln(C_e)+3.2662$	0.9838	26.2115	6.4851
Ho	$\ln(q_e)=0.1808\ln(C_e)+2.3297$	0.9950	10.2794	5.5310
Yb	$\ln(q_e)=0.7722\ln(C_e)+2.9209$	0.9828	18.5580	1.2950
Lu	$\ln(q_e)=0.4854\ln(C_e)+2.8683$	0.9444	17.6071	2.0602
Y	$\ln(q_e)=0.6547\ln(C_e)+2.1791$	0.9025	8.8383	1.5274
Sc	$\ln(q_e)=0.3962\ln(C_e)+2.2898$	0.9429	9.8730	2.5240

D-R model¹⁵

$$\ln Q_e = \ln Q_m - \beta \varepsilon^2$$

$$\varepsilon = RT \ln \left(1 + \frac{1}{C_e} \right)$$

$$E = (2\beta)^{-0.5}$$

Where β was a constant ($\text{mol}^2 \cdot \text{J}^{-2}$) and related to adsorption energy; Q_m was the theoretical saturated adsorption capacity ($\text{mg} \cdot \text{g}^{-1}$); ε was Polanyi potential; R was gas constant ($8.314 \text{ J} \cdot \text{mol}^{-1} \cdot \text{K}^{-1}$), T was the absolute temperature (K); E was the average adsorption energy ($\text{kJ} \cdot \text{mol}^{-1}$) and represented the energy required to transfer 1 mol of metal ions from the solution to the surface of the solid phase. The value of E could reflect whether the adsorption mechanism was a physical reaction or a chemical reaction. When $E > 8 \text{ kJ} \cdot \text{mol}^{-1}$, the adsorption process follows chemical adsorption, while $E < 8 \text{ kJ} \cdot \text{mol}^{-1}$, the adsorption process was a physical reaction.

Table S7. The result of data processing according to D-R model

Elements	Equation	R ²	Parameter		
			β ($\text{mol}^2 \cdot \text{J}^{-2}$)	E ($\text{kJ} \cdot \text{mol}^{-1}$)	Q_{max} ($\text{mg} \cdot \text{g}^{-1}$)
Nd	$\ln(Q_e) = 3.6081 - 8.001 \times 10^{-9} \varepsilon^2$	0.9543	8.001×10^{-9}	15.81	36.8959
Sm	$\ln(Q_e) = 3.2104 - 1.137 \times 10^{-8} \varepsilon^2$	0.9574	1.137×10^{-8}	13.26	24.7890
Eu	$\ln(Q_e) = 3.4517 - 2.801 \times 10^{-8} \varepsilon^2$	0.953	2.801×10^{-8}	8.45	31.5540
Ho	$\ln(Q_e) = 2.6778 - 1.200 \times 10^{-8} \varepsilon^2$	0.9603	1.200×10^{-8}	12.91	14.5530

Yb	$\ln(Q_e) = 3.4329 - 3.197 \times 10^{-8} \cdot C_e$	0.9578	3.197×10^{-8}	7.91	30.9663
Lu	$\ln(Q_e) = 3.4410 - 2.000 \times 10^{-8} \cdot C_e$	0.9569	2.000×10^{-8}	10.00	31.2182
Y	$\ln(Q_e) = 2.8273 - 4.001 \times 10^{-8} \cdot C_e$	0.9555	4.001×10^{-8}	7.07	16.8998
Sc	$\ln(Q_e) = 2.6359 - 1.600 \times 10^{-8} \cdot C_e$	0.9666	1.600×10^{-8}	11.18	13.9559

Tempkin model ¹⁶

$$Q_e = B_T \ln K_T + B_T \ln C_e$$

Where the value of the B_T was calculated from the following equation: $B_T = (RT)/b_T$, R was the gas constant ($8.314 \text{ J} \cdot \text{mol}^{-1} \cdot \text{K}^{-1}$), b_T was the Tempkin constant ($\text{J} \cdot \text{mol}^{-1}$) and related to adsorption heat. K_T was the equilibrium binding constant ($\text{L} \cdot \text{g}^{-1}$) and related to the maximum binding energy.

Table S8. The result of data processing according to Tempkin model

Elements	Equation	Parameter		
		R ²	B _T	K _T
Nd	$Q_e = 9.0897 \ln C_e + 37.799$	0.8545	9.0897	63.9718
Sm	$Q_e = 3.8971 \ln C_e + 19.61$	0.9702	3.8971	153.2310
Eu	$Q_e = 7.7306 \ln C_e + 21.578$	0.9665	7.7396	16.2485
Ho	$Q_e = 2.2484 \ln C_e + 10.392$	0.9805	2.2484	101.6925
Yb	$Q_e = 8.0659 \ln C_e + 20.264$	0.9395	8.0659	12.3333
Lu	$Q_e = 7.9296 \ln C_e + 23.234$	0.9650	7.9196	18.7977
Y	$Q_e = 3.4884 \ln C_e + 9.9655$	0.8066	3.4884	17.4049
Sc	$Q_e = 2.3076 \ln C_e + 10.189$	0.8240	2.3076	82.7157

Table S9. 16 kinds of REEs linear standard curve

Elements		R ²	Liner range
La	$Y = 242.396X + 190.248$	0.99969	5~1000 μg/L
Ce	$Y = 41.843X + 23.1529$	0.99986	5~1000 μg/L
Pr	$Y = 33.372X + 32.615$	0.99997	5~1000 μg/L
Nd	$Y = 29.463X + 214.024$	0.99781	5~1000 μg/L
Sm	$Y = 53.289X - 17.493$	0.99986	5~1000 μg/L
Eu	$Y = 120.374X + 23.768$	0.99999	5~1000 μg/L
Gd	$Y = 73.411X + 38.238$	0.99996	5~1000 μg/L
Tb	$Y = 49.724X + 14.738$	0.99995	5~1000 μg/L
Dy	$Y = 83.063X + 0.00$	0.99784	10~1000 μg/L
Ho	$Y = 35.289X + 17.842$	0.99996	5~1000 μg/L
Er	$Y = 54.089X + 2.625$	0.99999	5~1000 μg/L
Tm	$Y = 139.274X + 34.453$	1.00000	5~1000 μg/L
Yb	$Y = 611.496X + 120.269$	1.00000	5~1000 μg/L

Lu	$Y=213.229X+1.236$	0.99999	5~1000 $\mu\text{g/L}$
Y	$Y=152.899X+74.869$	0.99998	5~1000 $\mu\text{g/L}$
Sc	$Y=487.212X+5.708$	0.99999	5~1000 $\mu\text{g/L}$

Table S10. Comparison of the $\text{Fe}_3\text{O}_4@\text{mSiO}_2\text{-DODGA}$ with the other conventional materials

Entry	Materials	Recycling times	REEs	Ref.
		The final adsorption ratio		
1	$\text{Fe}@CS\text{-DGA}$	5/>90%	Pb(II)	28
2	$\text{Fe}_3\text{O}_4@\text{TODGA}$	3/80%, 92%	Am(III), Pu(IV)	29
3	$\text{Fe}_3\text{O}_4@\text{HA-MNPs}$	6/95%	Eu(III)	23
4	SBA-15-BSEA- Fe_3O_4 -NPs	5/95%	Ce(III)	18

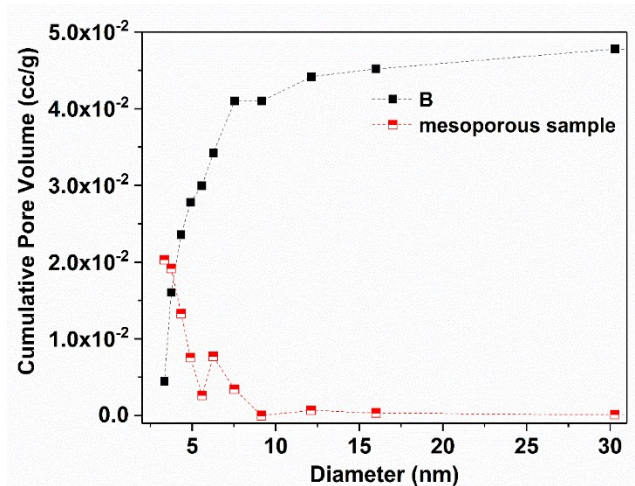


Figure S8. The pore diameter of $\text{Fe}_3\text{O}_4@\text{mSiO}_2\text{-DODGA}$

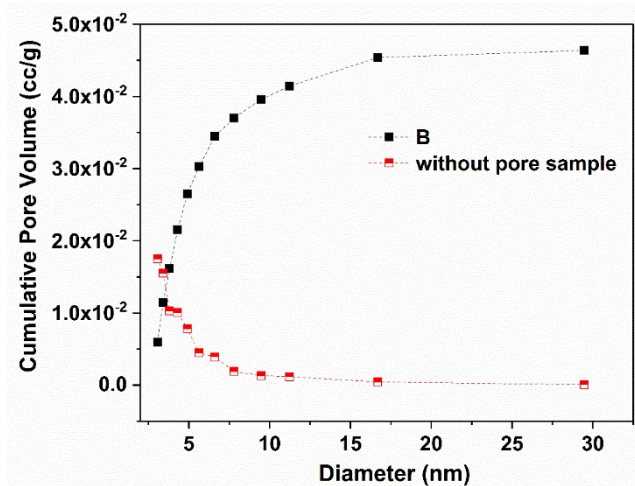


Figure S9. The pore structure of Fe₃O₄@SiO₂

Reference

- 1 S. W. Cao, Y. J. Zhu, J. Chang, *New J. Chem.*, 2008, **32**, 1526-1530.
- 2 J. Liu, Y. Sun, Y. Deng, Y. Zou, C. Li, X. Guo, L. Xiong, Y. Gao, F. Li and D. Zhao, *Angew. Chem.*, 2009, **48**, 5875-5879.
- 3 D. Liu, Y. Li, J. Deng and W. Yang, *React. Funct. Polym.*, 2011, **71**, 1040-1044.
- 4 J.P. Yang, F. Zhang, Y. R. Chen, S. Qian, P. Hu, W. Li, Y. H. Deng, Y. Fang, L. Han, M. Luqman, D. Y. Zhao, *Chem. Commun.*, 2011, **47**, 11618-11620.
- 5 Y. H. He, Y.Y. Huang, Y.L. Jin, X.J. Liu, G.Q. Liu and R. Zhao, *ACS Appl. Mater. Interfaces*, 2014, **6**, 9634-9642.
- 6 E. P. Horwitz, D. R. McAlister, A. H. Bond and R. E. Barrans Jr, *Solvent Extr. Ion Exc.*, 2005, **23**, 319-344.
- 7 G. Kantin, E. Chupakhin, D. Dar'in and M.Krasavin. *Tetrahedron Lett.*, 2017, **58**, 3160-3163.
- 8 M. Bessodes, N. Mignet. *Nanotechnology for Nucleic Acid Delivery*, 2013, **948**, 67-84.
- 9 N. A. Oladoja, C. O. Aboluwoye, Y. B. Oladimeji, *Turk J Eng Environ Sci*, 2008, **32**, 303-312.
- 10 Y.S. Ho, G. McKay, Sorption of dye from aqueous solution by peat. *Chem Eng J.*, 1998, **70**, 115-124
- 11 M. K. Sureshkumar, D. Das, M. B. Mallia and P. C. Gupta, *J. Hazard. Mater.*, 2010, **184**, 65-72.
- 12 S. H. Chein, W. R. Clayton. *Soil Sci. Soc. Am. J.*, 1980, **44**, 265-268.
- 13 E.,Repo, J. K. Warchol, T. A. Kurniawan and MET Sillanpää, *Chem Eng. J.* 2010, **161**, 73-82.
- 14 M. Jain, V. K.Garg, K. Kadirvelu, *J. Hazard. Mater.*, 2009, **162**, 365-372.
- 15 X.J. Hu, J.S. Wang, Y. G. Liu, X. Li, G.M. Zeng, Z. L. Bao, X. X. Zeng, A. W. Chen and F. Long, *J. Hazard. Mater.*, 2011, **185**, 306-314.
- 16 A. Sari, M. Tuzen, *J. Hazard. Mater.*, 2009, **164**, 1004-1011.